

Fiber based flexure sensor utilizing the sensitivity of evanescent coupling

B. Nelsen*^a, F. Rudek^a, Ch. Taudt^{abc}, T. Baselt^{abc}, P. Hartmann^{ac}

^aWestsächsische Hochschule Zwickau, Dr. Freidrich's Ring 2a, Zwickau, Germany;

^bTechnische Universität Dresden, Dresden, Germany;

^cFraunhofer-Institut für Werkstoff- und Strahltechnik IWS, 01277 Dresden, Germany

ABSTRACT

Sensing in harsh environments, such as in high magnetic fields like those found within MRI machines or in high-voltage conditions like those found within power transformers lends itself well for the use of fiber optic sensors. Where conventional electronic sensors fail for obvious reasons, specially designed fiber optic sensors can fill in these gaps. The aim of this research was to investigate the feasibility and technical parameters necessary to design a flexure sensor based on evanescent coupling between the modes of a two- (or more) core fiber. The design parameters are discussed and the sensitivity of the sensor is shown to be tunable by modifying variables which the coupling constant is sensitive to.

The physical model used to simulate this system is derived from an effective index change due to a combination of strain and an effective path difference which is induced by bending the fiber. The result of this model is a coupled-mode equation that can be systematically solved using an eigenvector approach to mode coupling. With proper fiber drawing techniques, this model predicts measurement sensitivities of curvature down to km^{-1} . Furthermore, this technique can be extended based on simulated long-wavelength measurements to make predictions about where along the length of the fiber the flexing took place. This system has the potential to be used as a competing system for Rayleigh backscattering based flexure measurements.

Keywords: Fiber optics, Flexure sensor, Coupled mode theory, Evanescent coupling, Hilbert space, Simulated long wavelength, Rayleigh backscattering

1. INTRODUCTION

Electronic sensors are always limited to certain environments because of some of their properties interact strongly with external conditions at minimum perturbing the result and at most destroying the sensor. Being susceptible to high voltages and to high magnetic fields, electric flexure sensors require a replacement in such extreme environments. This paper deals with the search for alternatives using optical fiber due to its inertness to high electric and magnetic fields. An evanescently coupled waveguide was selected to construct such a replacement sensor [1]. This was chosen because of its sensitivity to perturbations [2]. This paper is a theoretical investigation into the mechanisms that govern the coupling between the two cores, including the interaction of the cores with both construction parameters and under the influence of strain [3,4].

Rayleigh backscattering is the gold standard used at the moment to detect strain in fibers [5]. It provides information such as microstrains and how far down a fiber these microstrains occur [6]. However, most of the implementations require highly sensitive detectors and a tunable laser source. This makes the sensor both expensive and complex. In this paper, we will present ways based on an evanescently coupled multicore fiber which could provide an alternative sensor to Rayleigh backscattering sensors.

*Bryan.Nelsen@fh-zwickau.de; phone +49 0 375 5361587

2. MATHEMATICAL DESCRIPTION OF THE SENSOR

2.1 Hilbert space solutions to the wave equation

In this section, a short discussion will be given on transforming the wave equation into a form easily described in Hilbert space. With the basic assumption of time independence and translational invariance along the propagation direction, or z -direction of the fiber, the wave equation is very easily cast into the common form

$$\nabla_T^2 E_z + ((nk_o)^2 - \beta^2)E_z = 0. \quad (1)$$

Here the subscript T represents the transverse direction to the direction of propagation, n is the cross-sectional index of refraction profile and k_o is the free-space wavevector and β is the propagation constant. For a single-core step index fiber similar to the ones we are considering in this paper, the general form of the eigenvalue solutions is calculated in cylindrical coordinates and is of the form [7]

$$E_z^{l,m} = \left(J_m(k_{l,m}r)(1 - \Theta(r - a)) + A_{l,m}K_m(\gamma_{l,m}r)\Theta(r - a) \right) e^{im\varphi}, \quad (2)$$

with l and m being the radial and angular quantum numbers respectively, with J_m and K_m being the Bessel function of the first kind and modified Bessel function of the second kind respectively, $k_{l,m}$ and $\gamma_{l,m}$ are the transverse components of the wavevector both inside and outside the fiber, $A_{l,m}$ is a constant for continuity across the core-cladding boundary and $\Theta(r - a)$ is the Heaviside step function which defines the core-cladding boundary. It is possible to generate the transverse components of the electric field using Maxwell equations, but a full vector analysis is not needed for the scope of this paper and is therefore ignored. The elegant fact about Eq. (1) is that it lends itself well for expanding the notation into a Hilbert space calculation for the purpose of calculating both small and large tangential perturbations to the index of refraction, i.e.

$$\hat{H}|\psi_z^{l,m}\rangle = \beta_{l,m}^2|\psi_z^{l,m}\rangle \quad (3)$$

with

$$\hat{H} = (\hat{K} + \hat{P}) = (\nabla_T^2 + (nk_o)^2). \quad (4)$$

This notation was used because the equation closely resembles that of the quantum-mechanical Hamiltonian with $\hat{K} = \nabla_T^2$ and $\hat{P} = (nk_o)^2$ and $|\psi_z^{l,m}\rangle$ being the properly normalized electric field in abstract vector space. Projected back into Cartesian space the ‘wavefunction’ looks like:

$$\langle \vec{x}_T | \psi_z^{l,m} \rangle = E_z^{l,m} = \left(J_m(k_{l,m}r)(1 - \Theta(r - a)) + A_{l,m}K_m(\gamma_{l,m}r)\Theta(r - a) \right) e^{im\varphi}. \quad (5)$$

Here, $|\vec{x}_T\rangle$ is the transverse spatial coordinate system representation in Hilbert space. These modes are, however, orthogonal and follow the relationship

$$\langle \psi_z^{l',m'} | \psi_z^{l,m} \rangle = \delta_{l,l'}\delta_{m,m'} \quad (6)$$

with $\delta_{l,l'}$ being the Kronecker delta. It is worth noting that these modes of the fiber do not form a complete basis because we were only searching for bound states.

Consideration of the cladding modes must also be taken into account if one wants to use the completeness relation, as such

$$\sum_{l,m} |\psi_z^{l,m}\rangle \langle \psi_z^{l,m}| + \sum_{clad} |\psi_{clad}\rangle \langle \psi_{clad}| = \mathbb{I}. \quad (7)$$

2.2 Evanescent coupling in Hilbert space

The basic idea of the evanescently coupled waveguide is that, in the cladding where the two modes behave as a dying exponential, the wavefunctions can no longer be thought of as independent. They have some overlap which mixes the two functions. An example of a coupled waveguide is shown in Fig. 1(a). These left and right waveguides each taken independently behave as if they are a single core fiber. Looking closer at the schematic in Fig. 1(b), it can be understood that $|\psi_L\rangle$ is the solution to the index profile when the core n_R is removed and $|\psi_R\rangle$ is the solution when the core n_L is removed.

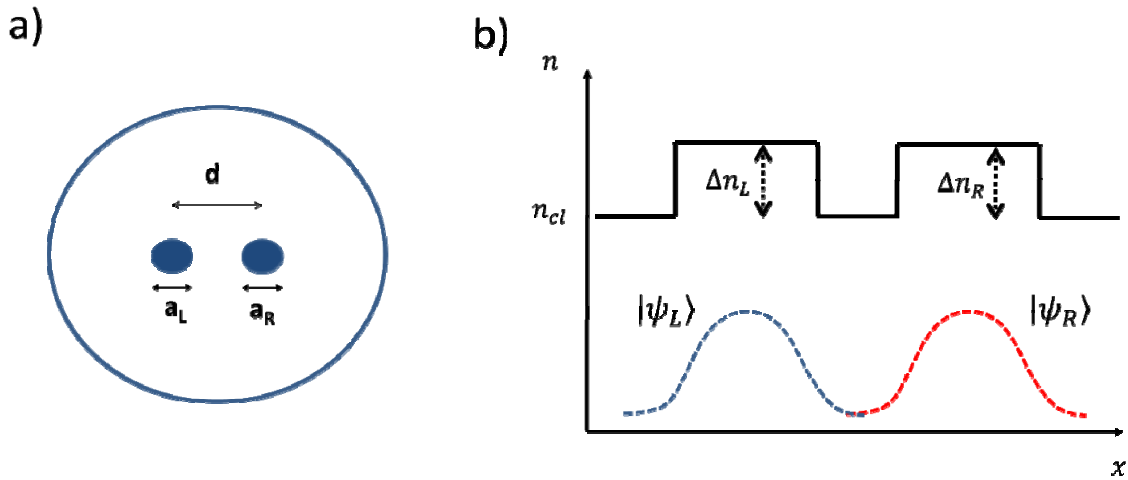


Figure 1. (a) schematic representation of the dual core evanescently coupled fiber considered here and (b) the cross-section of the index of refraction profile of (a) and the representative electric fields for each core independently.

Let $|\psi_L\rangle$ be the solution for core one and $|\psi_R\rangle$ be the solution for core two and let both cores only on their own only support a single mode. This assumption is only made to simplify the analysis, but could be relaxed if desired. Independently, they both satisfy their own eigenvalue equation for their respective potentials:

$$\hat{H}_L |\psi_L\rangle = \beta_L^2 |\psi_L\rangle \text{ and } \hat{H}_R |\psi_R\rangle = \beta_R^2 |\psi_R\rangle. \quad (8)$$

From this point on, it is worth noting that the cladding ‘potential’ can be subtracted from the individual Hamiltonians just as is done in similar vacuum renormalization calculations, i.e.

$$\hat{H}'_j = \hat{H}_j - (n_{cl} k_o)^2 \Rightarrow \beta_j^{2'} = \beta_j^2 - (n_{cl} k_o)^2, \quad (9)$$

with n_{cl} being the index of refraction of the cladding. In this way, we can easily express the new renormalized Hamiltonian in terms of the two independent renormalized Hamiltonians as:

$$\hat{H}' = \hat{K} + \hat{V}_L + \hat{V}_R = \hat{H}'_L + \hat{H}'_R - \hat{K}. \quad (10)$$

From this point on, an assumption has to be made. The spatial overlap between the states is what gives rise to the coupling as such:

$$\langle \psi_L | \psi_R \rangle = \int d^2 \vec{x}_T \psi_L^*(\vec{x}_T) \psi_R(\vec{x}_T) \equiv \frac{\Delta}{2} \quad (11)$$

However, to simplify the calculation, we must enforce that the overlap is small, i.e. $\Delta \ll 1$. We do this because we would like to write the Hamiltonian in terms of the ψ_L - and ψ_R - basis, but since the states are not orthogonal, it cannot be assumed in general that $|\psi_L\rangle\langle\psi_L| + |\psi_R\rangle\langle\psi_R| = \mathbb{I}$. In fact it can be shown that the orthogonalization of these states leads to

$$|\psi_L^n\rangle = \frac{1}{\sqrt{2}} \left[\left(\frac{\sqrt{1 + (1 - |\langle\psi_L|\psi_R\rangle|^2)}}{\sqrt{1 - |\langle\psi_L|\psi_R\rangle|^2}} \right) |\psi_L\rangle - \left(\frac{\langle\psi_R|\psi_L\rangle}{\sqrt{(1 + (1 - |\langle\psi_L|\psi_R\rangle|^2))(1 - |\langle\psi_L|\psi_R\rangle|^2)}} \right) |\psi_R\rangle \right] \quad (12)$$

and

$$|\psi_R^n\rangle = \frac{1}{\sqrt{2}} \left[\left(\frac{\sqrt{1 + (1 - |\langle\psi_L|\psi_R\rangle|^2)}}{\sqrt{1 - |\langle\psi_L|\psi_R\rangle|^2}} \right) |\psi_R\rangle - \left(\frac{\langle\psi_L|\psi_R\rangle}{\sqrt{(1 + (1 - |\langle\psi_L|\psi_R\rangle|^2))(1 - |\langle\psi_L|\psi_R\rangle|^2)}} \right) |\psi_L\rangle \right]$$

but when the overlap is relatively small, i.e. $\langle\psi_R|\psi_L\rangle \sim 0$, then the original states are orthogonal. So with the assumption that $|\psi_L\rangle\langle\psi_L| + |\psi_R\rangle\langle\psi_R| = \mathbb{I}$, the Hamiltonian \hat{H}' can be expanded as follows

$$\hat{H}' = \begin{pmatrix} \beta_L^{2'} + \langle\psi_L|\hat{V}_R|\psi_L\rangle & (\beta_L^{2'} + \beta_R^{2'}) \frac{\Delta}{2} - \langle\psi_L|\hat{K}|\psi_R\rangle \\ (\beta_L^{2'} + \beta_R^{2'}) \frac{\Delta^*}{2} - \langle\psi_R|\hat{K}|\psi_L\rangle & \beta_R^{2'} + \langle\psi_R|\hat{V}_L|\psi_R\rangle \end{pmatrix}. \quad (13)$$

Since we are working under the assumption that the overlap is small, the expectation values $\langle\psi_L|\hat{V}_R|\psi_L\rangle$ and $\langle\psi_L|\hat{K}|\psi_R\rangle$ are negligible and the final form of the Hamiltonian is

$$\hat{H}' = \begin{pmatrix} \beta_L^{2'} & (\beta_L^{2'} + \beta_R^{2'}) \frac{\Delta}{2} \\ (\beta_L^{2'} + \beta_R^{2'}) \frac{\Delta^*}{2} & \beta_R^{2'} \end{pmatrix}. \quad (14)$$

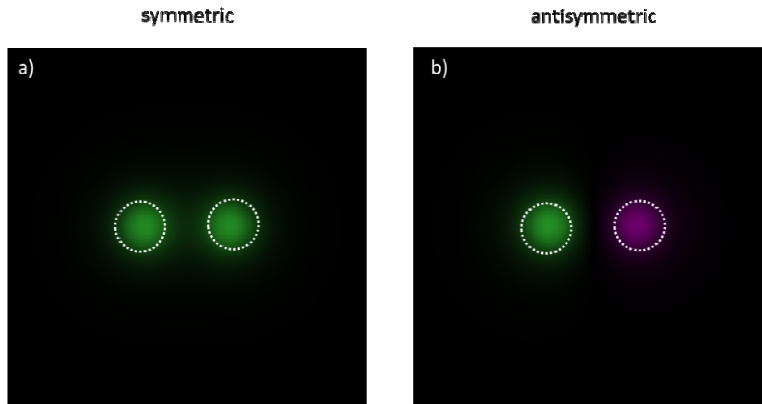


Figure 2. (a) Symmetric and (b) antisymmetric eigenfunctions of the evanescently-coupled dual core fiber. The dotted white circles represent the position of the cores and each single core has the properties given by the Thorlabs fiber 780HP. The center to center core separation is equal to two core diameters. The color represents the phase of the wave.

Let us for a moment consider the case of symmetry between the two cores when $\beta_L^{2'} = \beta_R^{2'} = \beta^{2'}$. The solution to the Hamiltonian becomes simple; that is

$$\hat{H}' = \beta^{2'} \begin{pmatrix} 1 & \Delta \\ \Delta^* & 1 \end{pmatrix}. \quad (15)$$

Therefore, after diagonalization

$$\beta_{\pm}^{2'} = \beta^{2'}(1 \pm |\Delta|), \quad (16)$$

$$|\psi_{-}\rangle = \frac{1}{\sqrt{2}}(|\psi_L\rangle + |\psi_R\rangle) \text{ and } |\psi_{+}\rangle = \frac{1}{\sqrt{2}}(|\psi_L\rangle - |\psi_R\rangle).$$

The symmetric field, $|\psi_{-}\rangle$, is shown in Fig. 2(a) and the antisymmetric field, $|\psi_{+}\rangle$, is shown in Fig. 2(b). These new modes represent the propagation independent modes of the system and can be used to predict coupling between the cores of the fiber. An interesting case to examine is what happens when light is injected into one core of the fiber, say the right core. This state can then be propagated down the length of the fiber using the propagator $e^{-i\beta z}$. This propagator is the same for any system with translational invariance. It is one of the main assumptions used to arrive at the results of Eq. 1.

As applied to the situation of the evanescently coupled wave guide with light coupled into the right core, it has this form:

$$|\psi(z)\rangle = e^{-i\beta_{+}z}|\psi_{+}\rangle\langle\psi_{+}|\psi_R\rangle + e^{-i\beta_{-}z}|\psi_{-}\rangle\langle\psi_{-}|\psi_R\rangle. \quad (17)$$

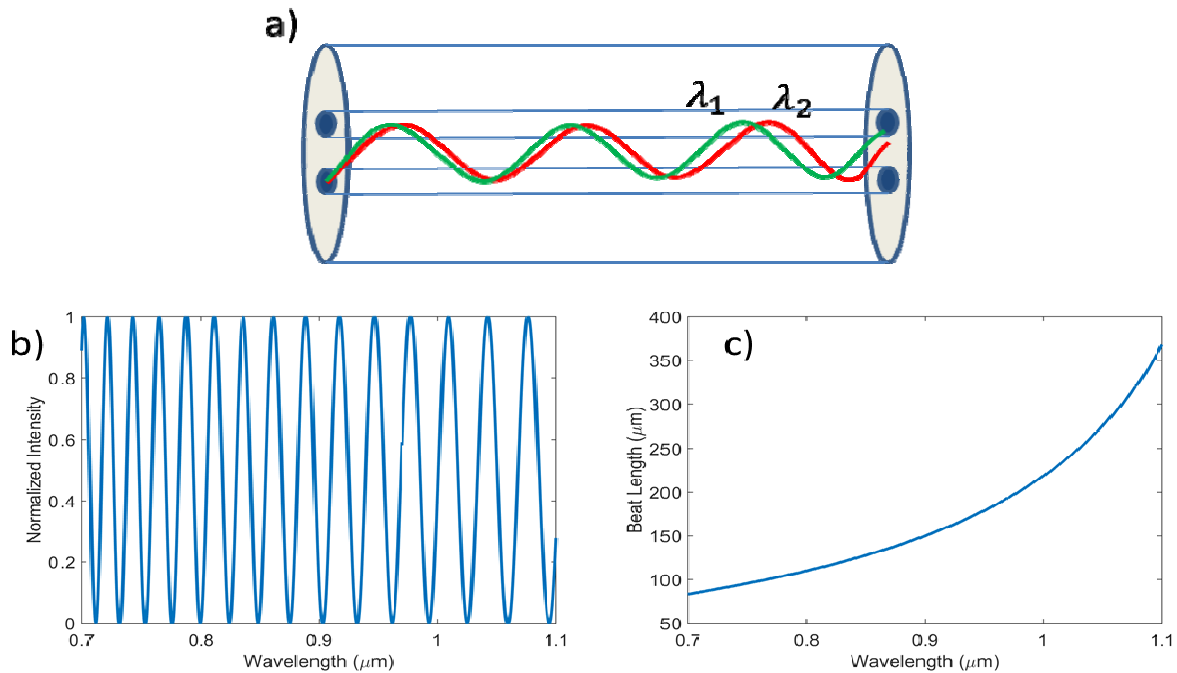


Figure 3. (a) Schematic representation of different wavelengths propagating with different phase velocities giving rise to a phase mismatch at the output of the fiber. (b) Intensity in the right core vs wavelength after propagating 200 mm down the same fiber shown in Fig. 2. (c) The beat length of the power in each core vs wavelength for fiber described in Fig. 2.

Looking at how much intensity remains in the right core after propagating some distance then is given by:

$$|\langle \psi_R | \psi(z) \rangle|^2 = \frac{1}{2} (1 + \cos((\beta_+ - \beta_-)z)). \quad (18)$$

Using the same parameters used to calculate the eigenfunctions in Fig. (2), Fig. 3(b) and Fig. 3(c) display the effects of Eq. 18 on the intensity output at the end of the fiber.

2.3 Effects of bending a fiber on the index of refraction

Strain in fiber optics is a well-studied problem. In particular, it has two strong effects which both have the same mathematical form but opposite signs. In order to generate the solutions for a bent fiber like that in Fig. 4, a reference frame that rotates with the fiber as the light travels down the fiber is used.

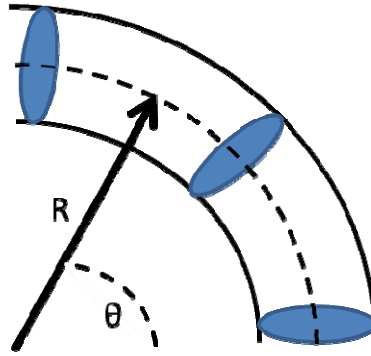


Figure 4. Representation of a bent fiber with a radius of curvature R pointing to center of the fiber. The cross-sectional circles represent the rotating coordinate system that the new eigenvalue equation is written in in order to solve the for the propagation independent modes of the fiber.

This reference frame is illustrated in Fig. 4 as the cross-sectional circles. Under this coordinate transformation, the standard wave equation, Eq. 1, becomes

$$\nabla_T^2 E_z + \left(n^2 \left(1 + 2 \frac{x}{R} \right) k_o^2 - \beta^2 \right) E_z = 0. \quad (19)$$

Besides this main effect, the strain inside the crystal due to compression and extension causes a small, but non-negligible contribution to the wave equation. Thankfully, this index of refraction profile has the same symmetry as the change due to the coordinate transformation and we wind up with a wave equation

$$\nabla_T^2 E_z + \left(n^2 \left(1 + 2 \frac{x}{R_{\text{eff}}} \right) k_o^2 - \beta^2 \right) E_z = 0, \quad (20)$$

where ($R_{\text{eff}} = 1.41R$) is the radius seen in Fig. 4, but scaled by strain effects. The elegant part of this solution is that a bend of the fiber is the same as adding a linear offset to the index of refraction of the fiber (see Fig. 5). The solution is, based on the Hamiltonian style math we used earlier, mostly trivial and this wave equation can be solved in a similar fashion to Eq. 10 by expanding it in the basis given by solving the unperturbed Hamiltonian, i.e.

$$\hat{H} = \sum_{i,j} |\psi_i\rangle \langle \psi_i| \hat{H}_o + 2(nk_o)^2 \frac{\hat{x}}{R_{\text{eff}}} |\psi_j\rangle \langle \psi_j|. \quad (21)$$

As was mentioned in Eq. (6), the expansion of this Hamiltonian must include the cladding states. It is especially important in this case because fiber bending losses are due to the coupling between eigenstates of the core and cladding.

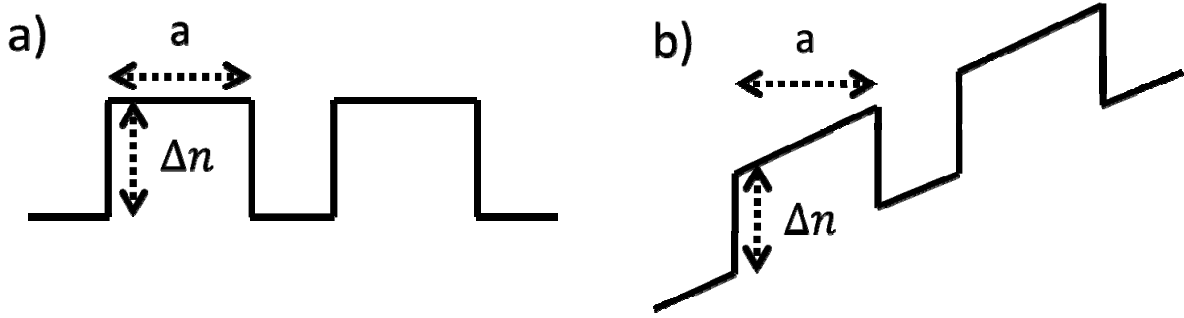


Figure 5. Schematic depicting the index of refraction (a) before strain and (b) after strain.

2.4 Evanescent coupling under flexure

Combining Eq. (14) dealing with the Hamiltonian for a coupled core fiber and Eq. (21) adding in the perturbation due to straining the fiber gives a new Hamiltonian

$$\hat{H}' = \begin{pmatrix} \beta_L^{2'} + 2 \frac{(nk_o)^2}{R_{\text{eff}}} \langle \psi_L | \hat{x} | \psi_L \rangle & (\beta_L^{2'} + \beta_R^{2'}) \frac{\Delta}{2} \\ (\beta_L^{2'} + \beta_R^{2'}) \frac{\Delta^*}{2} & \beta_R^{2'} + 2 \frac{(nk_o)^2}{R_{\text{eff}}} \langle \psi_R | \hat{x} | \psi_R \rangle \end{pmatrix}. \quad (22)$$

The off-diagonal elements due to the strain perturbation are zero because of symmetry reasons. Assuming that $|\psi_L\rangle$ and $|\psi_R\rangle$ are almost the same function and the two cores are symmetrically located an equal distance about the center of the fiber, we can replace them with the position of the center of the core, or from Fig. 1(a) $\pm d/2$. Equation (22) then simplifies to

$$\hat{H}' = \begin{pmatrix} \beta_L^{2'} - \frac{(nk_o)^2}{R_{\text{eff}}} d & (\beta_L^{2'} + \beta_R^{2'}) \frac{\Delta}{2} \\ (\beta_L^{2'} + \beta_R^{2'}) \frac{\Delta^*}{2} & \beta_R^{2'} + \frac{(nk_o)^2}{R_{\text{eff}}} d \end{pmatrix}. \quad (23)$$

The solution to this Hamiltonian is expressible in closed form like

$$\beta_{\pm}^{2'} = \frac{\beta_L^{2'} + \beta_R^{2'}}{2} \pm \frac{1}{2} \sqrt{\left(\beta_R^{2'} - \beta_L^{2'} + 2 \frac{(nk_o)^2}{R_{\text{eff}}} d \right)^2 + (\beta_L^{2'} + \beta_R^{2'})^2 |\Delta|^2}, \quad (24)$$

and the new eigenstates of the system become

$$|\psi_{-}\rangle = (L_{+}|\psi_{L}\rangle + R_{+}|\psi_{R}\rangle) \text{ and } |\psi_{+}\rangle = (R_{+}|\psi_{L}\rangle - L_{+}|\psi_{R}\rangle)$$

with

$$L_{+} = \frac{\beta_{+}^{2'} - \beta_{-}^{2'}}{\sqrt{(\beta_{L}^{2'} + \beta_{R}^{2'})^2 |\Delta|^2 / 4 + (\beta_{+}^{2'} - \beta_{-}^{2'})^2}} \quad (25)$$

and

$$R_{+} = \frac{(\beta_{L}^{2'} + \beta_{R}^{2'}) |\Delta| / 2}{\sqrt{(\beta_{L}^{2'} + \beta_{R}^{2'})^2 |\Delta|^2 / 4 + (\beta_{+}^{2'} - \beta_{-}^{2'})^2}}$$

3. THE SENSOR DESIGN AND FUNCTION

The sensor design is based on the theory in the above sections where an evanescently coupled waveguide is designed with two slightly different cores. The cores of the fiber should be significantly different such that when light is launched into one core, the propagation constants are different enough to prevent strong coupling from one core to the other. When a flexure perturbation to the fiber is applied, the propagation constants will shift and the two cores will be brought into resonance. Some percentage of the light will couple from one core into the other. Based on the different propagation constants in the two cores, the time of flight from the light coupled into the 2nd core will be different than from the light that remains in the initial core and the position that the flexure was applied along the fiber should be able to be deduced.

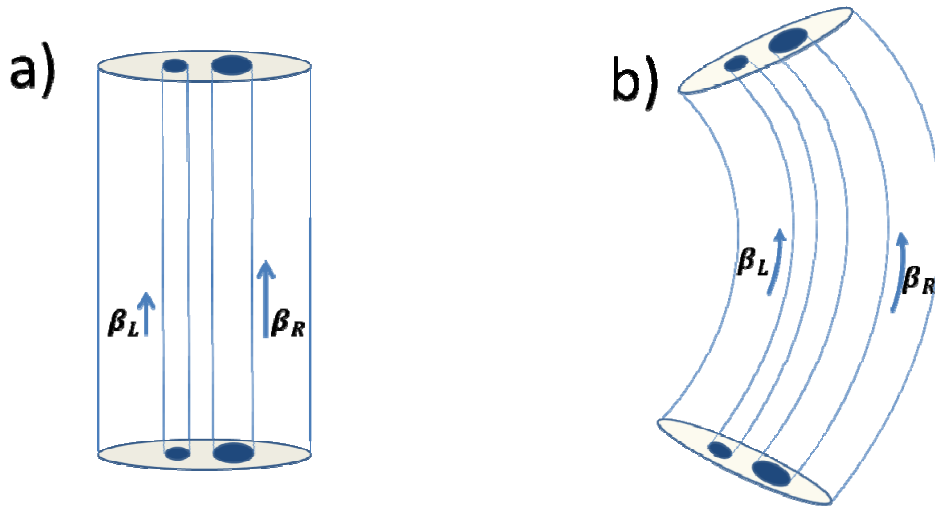


Figure 6. (a) Mismatch in propagation constant between the two cores when fiber is unperturbed. This disrupts the coupling and does not allow light to transfer between cores. (b) Bending the fiber changes the effective propagation constants so they are closer to match. This allows light to couple from one core to the other.

4. CONCLUSIONS

The search for a fiber-based sensor to detect flexure in harsh environments led this research in the direction of evanescently coupled wave guides. The equation governing evanescent coupling was written down in a Hilbert space construction. This made it relatively easy to add in a mathematical analysis based on the flexing the sensor. The flexure calculation took the variables of both strain and path changes into account when modeling this system. Based on the underlying physics taken away from this analysis, a fiber design was proposed that should enable the measurement of both the amount of flexure and the position that flexure took place. A more rigorous analysis of the full design is still called for based on the mathematical model derived within this paper.

ACKNOWLEDGMENTS

The authors want to thank the Federal Ministry of Education and Research for financial support under grant number 16SV7095 as well as the members of the optical technologies working group at the West Saxon University of Applied Sciences Zwickau for fruitful discussions.

REFERENCES

- [1] Schiffner, G., Schneider, H., Schöner, G., "Double-Core Single-Mode Optical Fiber as Directional Coupling," *Appl. Phys.* 23, 41-45 (1980).
- [2] Okamoto, K., [Fundamentals of Optical Waveguides], 2nd Ed., Academic Press – Elsevier, Chpt. 1 (2006)
- [3] Guzman-Sepulveda, J.R., May-Arrijoja, D.A., "In-fiber directional coupler for high-sensitivity curvature measurement," *Optics Express* 21(10), 11853-11861 (2013).
- [4] Guzman-Sepulveda, J.R., Guzman-Cabrera, R., Tores-Cisneros, M., Sanchez-Mondragon, J.J., May-Arrijoja, D.A., "A Highly Sensitive Fiber Optic Sensor Based on Two-Core Fiber for Refractive Index Measurement," *Sensors*, 13, 14200-14213 (2013)
- [5] Gold, M., "On the theory of backscattering in single-mode optical fibers," *Journal of Lightwave Technology* 2, 76-82 (1984).
- [6] Froggatt, M., Moore, J., "High-spatial-resolution distributed strain measurement in optical fiber with Rayleigh scatter," *Appl. Opt.* 37(10), 1735-1740 (1998)
- [7] Iizuka, K., [Elements of Photonics, Volume II: For Fiber and Integrated Optics], John Wiley & Sons, Inc., 709-739 (2002)